A Field Goniometer System (FIGOS) for Acquisition of Hyperspectral BRDF Data

Stefan R. Sandmeier and Klaus I. Itten, *Senior Member, IEEE*

***Abstract*— A new field goniometer system (FIGOS) is introduced that allows *in situ* measurements of hyperspectral bidirectional reflectance data under natural illumination conditions. Hyperspectral bidirectional reflectance distribution function (BRDF) data sets taken with FIGOS nominally cover the spectral range between 300 and 2450 nm in 704 bands. Typical targets are small-growing, dense, and homogeneous vegetation canopies, man-made surfaces, and soils. Field BRDF data of a perennial ryegrass surface reveal a strong spectral variability. In the blue and red chlorophyll absorption bands, BRDF effects are strong. Less-pronounced bidirectional reflectance effects are observed in the green and in most of the near-infrared range where surface reflectance is high. An anisotropy index (ANIX), defined as the ratio between the maximum and minimum bidirectional reflectance over the hemisphere, is introduced as a surrogate measurement for the extent of spectral BRDF effects. The ANIX data of the ryegrass surface show a very high correlation with nadir reflectance due to multiple scattering effects. Since canopy geometry, multiple scattering, and BRDF effects are related, these findings may help to derive canopy architecture parameters, such as leaf area index (LAI) or leaf angle distribution (LAD) from remotely sensed hyperspectral BRDF data. Furthermore, they show that normalized difference vegetation index (NDVI) data are strongly biased by the spectral variability of BRDF effects.**

***Index Terms*—BRDF, goniometer, hyperspectral.**

I. Introduction

GONIOMETERS have been used to measure angles and provide exact angular reference systems for many hundreds of years in a wide variety of disciplines [1]. Originally designed for surveying and navigational applications, they became increasingly important in remote-sensing science with the growing recognition of the bidirectional reflectance distribution function (BRDF) [2]. The BRDF is a theoretical concept that describes the directional reflectance phenomena by relating the incident irradiance from one given direction to its contribution to the reflected radiance in another specific direction. Bidirectional effects are intrinsic and distinctive surface characteristics that affect all ground and remotely sensed radiation data.

Manuscript received February 25, 1998; revised July 27, 1998. The work of S. R. Sandmeier was supported by the Swiss National Science Foundation (8220-050392) and the Universities Space Research Association of the United States through NASA/Goddard Visiting Scientist Program NAS-5-32484. The transportation unit was supported in part by "Stiftung für wiss. Forschung an der Universität Zürich."

S. R. Sandmeier was with Remote Sensing Laboratories, Department of Geography, University of Zürich, Zürich, Switzerland. He is now with Biospheric Sciences Branch, NASA/Goddard Space Flight Center, Greenbelt, MD 20771 USA (e-mail: sandi@geo.unizh.ch).

K. I. Itten is with the Remote Sensing Laboratories, Department of Geography, University of Zürich, CH-8057 Zürich, Switzerland.

Publisher Item Identifier S 0196-2892(99)01183-3.

Early measurements of bidirectional reflectance over various vegetation and soil surfaces demonstrated that most terrestrial surfaces expose non-Lambertian, i.e., anisotropic, reflectance characteristics [3]–[5]. As a result researchers identified the need for a more complete characterization of the BRDF effect as a key research issue in the early 1980's. Subsequently, more sophisticated goniometers have been developed, such as the portable apparatus for rapid acquisition of bidirectional observations of the land and atmosphere, PARABOLA. This unique three-band radiometer is able to scan almost a complete sphere in a helical pattern and provides a multitude of bidirectional reflectance data over a wide range of natural surfaces [6]. Goniometric devices have also been used to calibrate field reference–reflectance panels to compensate for their non-Lambertian BRDF characteristics [7], [8]. Today, the anisotropy of radiation scattered from natural and man-made surfaces is well accepted, and a large number of models have been developed to describe adequately the bidirectional reflectance effect of various surfaces. However, most of the bidirectional reflectance data currently available lack a high spectral resolution, and most BRDF models do not explicitly take the spectral variability of BRDF effects into account.

Both NASA and the European Space Agency (ESA) have recognized the potential of combining multidirectional and hyperspectral reflectance data [9], [10], and with the advent of MODIS on NASA's Earth Observing System (EOS) AM-1 platform in 1999, high spectral resolution data with significant bidirectional effects will become widely available. In addition, remote-sensing companies and military agencies are currently developing satellite systems with high and hyperspectral resolution and off-nadir tilting capability, such as Warfighter-1 on OrbView-4 [11] and the multispectral high-resolution system (MSRS) on DAVID [12]. The potential of these new sensors can only be fully assessed if the physics driving spectral BRDF effects are well understood and if high-spectral ground BRDF data are available to validate the various BRDF model approaches.

The spectral variability of BRDF effects in vegetation canopies has been previously alluded to by Kimes [5], but as in the PARABOLA studies of Deering *et al.* [13], the phenomenon could not fully be addressed mainly due to a lack of high-spectral resolution data. Russell *et al.* [14], [15] and Ranson *et al.* [16] used hyperspectral airborne BRDF data from the advanced solid-state array spectroradiometer (ASAS) to focus on the view and illumination angle dependence of the BRDF rather than on the spectral variability. Middleton [17] analyzed nadir-normalized hyperspectral BRDF data of

Fig. 1. FIGOS field goniometer assembled with the GER-3700 spectroradiometer for a field campaign at the University of Zürich campus.

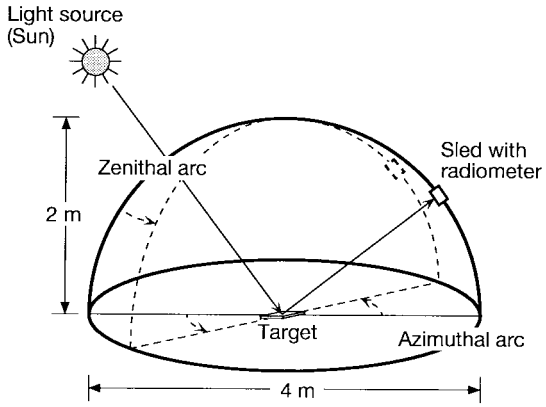

Fig. 2. Dimensions and design of FIGOS.

Fig. 3. Overview of FIGOS showing the PC control unit for the GER-3700 sensor (on the left), the spectralon reference panel (in the foreground), and the trailer used for transporting FIGOS (in the background).

Fig. 4. Setup of the trailer with the disassembled FIGOS components.

moderately sparse Konza prairie grass to elucidate spectral BRDF effects in vegetation canopies, but the influence of the soil background on the grass reflectance measurements affected the spectral characteristics of the grass BRDF.

In this study, BRDF measurements acquired in a field experiment over a dense ryegrass surface (i.e., no soil surface contributions) are analyzed for the persistence of the spectral variability of BRDF effects and for the relationship between BRDF effects, nadir reflectance signature, and multiple scattering effects. The data are obtained with a newly developed field goniometer system (FIGOS) that enables the acquisition of hyperspectral BRDF data and the investigation of spectral BRDF effects at small scales.

II. Instrument Description

A. Design and Performance

The field goniometer system (FIGOS) was designed and built by W. Sandmeier at Fa. Lehner & Co. AG, Gränichen, Switzerland, in joint operation with the Remote Sensing Laboratories (RSL) at the University of Zürich, Switzerland. FIGOS is a transportable field goniometer that is currently operated with a PC-controlled GER-3700 spectroradiometer covering the spectrum between nominal 300 and 2450 nm in 704 bands with a resolution of 1.5 (300–1050 nm) and 8.4 nm (1050–2450), respectively [18] (Fig. 1). The goniometer consists of three major parts: a zenith arc and an azimuth rail, each of 2-m radius, and a motorized sled, where the sensor is mounted (Fig. 2). All parts are made of black-coated aluminum, resulting in a total weight of only 230 kg. The complete goniometer system is stored and transported on a trailer with a specifically designed interior, allowing fast and convenient access to a field site (Figs. 3 and 4). For transportation, the azimuth rail and the zenith arc are disassembled. Mounting of the zenith arc is provided by sleds connected to the azimuth rail that allow a full 360° rotation. The ball-bearings of the wagons embrace the azimuth rail in a way that the zenith arc is tightly fixed so that measurements can be taken even on sloped terrain. A support linking the center of the zenith arc with the azimuth rail provides further stabilization and helps to guide the cables (Fig. 3). In order to enable measurements in the solar principal plane, the zenith arc is mounted eccentrically on the azimuth rail and only the radiometer itself moves in the principal plane (Fig. 1). Since the radiometer's instantaneous field-of-view is rather small, nominal 3° (circular shape), and always pointing to the center of the hemisphere, shadow on the target area only occurs when the radiometer is aligned with the sun. Mounted on the goniometer, the sensor's footprint is about 10.5 cm (diameter) in nadir direction and about 41 cm (major axis) in the most extreme view zenith angle position of 75° (Fig. 5). Thus, the

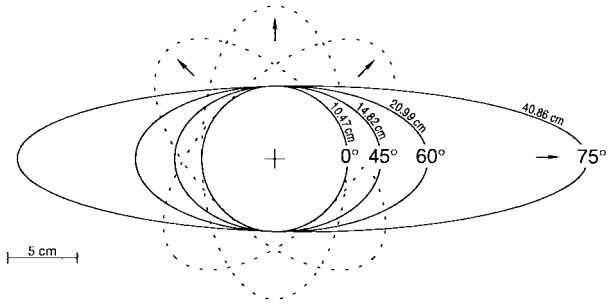

Fig. 5. Footprint area of the sensor's field-of-view for various view zenith angle positions. The arrows indicate the viewing direction of the radiometer. The dotted lines show three different view azimuth angles for a constant view zenith angle of 60°.

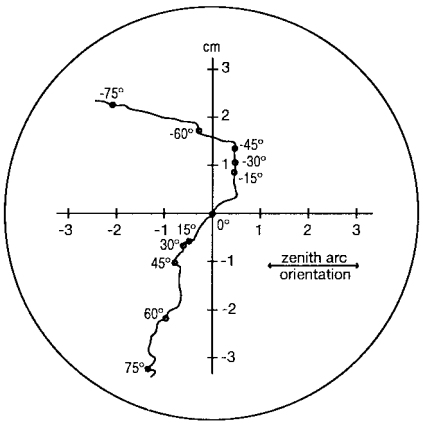

Fig. 6. Track of a laser, representing the center of the sensor's field-of-view, moving over the zenith arc. The coordinate system is aligned to the center of the azimuth circle.

radiometer is always viewing approximately the same surface area in the center of the hemisphere.

The sled with the spectroradiometer mounted is driven by a 24-V DC braking motor, and a precision chain serves as a guideway for the 3/8″ cogwheel. The motor velocity is set to 2.5°/s. Fully adjustable labels on the zenith arc allow for an automated positioning of the spectroradiometer. It is also possible to drive the sled-motor manually from a remote control unit to any desired position on the zenith arc between −75 and +75°. Positioning precision on the zenith arc is within ±0.2°. The geometric precision of the zenith arc is referenced with the help of a laser moving over the zenith arc on plane ground. The deviation of the laser spot, representing the center of the sensor's field-of-view, shows values within ±3.5 cm (Fig. 6). The roundness of the zenith arc is nearly perfect, showing deviations of the laser spot from the center within ±1 cm between −60 and +60°. The azimuth view angle is given by a scale engraved in the azimuth basement. Currently, the zenith arc is positioned manually with the help of a pointer and a brake fixing the position of the zenith arc. The azimuth arc is almost perfectly round. A laser spot pointing vertically from the center of the zenith arc on the ground moves less than ±1 cm when the zenith arc is rotated.

In the most current configuration, the PC control unit for the spectroradiometer is attached to a rod linking the zenith and azimuth arcs (Fig. 3). By this means, the PC and connected cables are rotated with the zenith arc, which greatly reduces the risk of a cable jam and facilitates the operation of FIGOS. About 90 min are needed for the setup of the goniometer with a team of two people. An illustration of the assembling steps is given in Sandmeier *et al.* [19].

TABLE I
ESTIMATED COSTS AND FINANCIAL RESOURCES FOR FIGOS

Item	*Sponsor*	*Cost **
Proposal, idea and design	Remote Sensing Laboratories	21'000.-
Development and construction	Max Lehner + Co. AG, CH-5722 Gränichen; Willy Sandmeier	40'000.-
Material	Remote Sensing Laboratories	10'000.-
Manufacturing	Max Lehner + Co. AG, CH-5722 Gränichen;Willy Sandmeier	90'000.-
Transportation unit	Max Lehner + Co. AG, CH-5722 Gränichen; Stiftung für wiss. Forschung an der Universität Zürich	14'000.-
Total		175'000.-

* Costs are estimates of Lehner+Co. AG made in Swiss Francs; 1 Swiss Franc equals about 0.7 US Dollar.

B. Construction Schedule and Costs

The main construction phase ran from October 1993 to May 1994 and was followed by a two-month period of initial tests. In April 1995, a first field experiment with a GER-3700 spectroradiometer was performed. In 1996, FIGOS became fully operational with the purchase of a trailer for storing and transporting the goniometer parts. The planning and main construction of FIGOS required about 700 working hours. The estimated costs are listed in Table I.

III. METHODOLOGY

A. Definitions

1) BRDF: The bidirectional reflectance distribution function (BRDF) $f_r[sr^{-1}]$, as defined by Nicodemus *et al.* [2], is the ratio of the radiance dL_r $[\mathrm{W}\cdot\mathrm{m}^{-2}\cdot sr^{-1}\cdot\mathrm{nm}^{-1}]$ reflected in one direction (θ_r, φ_r) to the incident irradiance dE_i $[\mathrm{W}\cdot\mathrm{m}^{-2}\cdot\mathrm{nm}^{-1}]$ from direction (θ_i, φ_i) (Fig. 7)

$$f_r(\theta_i, \varphi_i; \theta_r, \varphi_r; \lambda) = \frac{dL_r(\theta_i, \varphi_i; \theta_r, \varphi_r; \lambda)}{dE_i(\theta_i, \lambda)}. \quad (1)$$

Although dL_r and dE_i are both clearly directional quantities, BRDF measurements are given in sr^{-1}. This is due to diffuse reflection, which causes the small, but finite incident irradiance dE_i to be reflected in infinitesimally small solid angles in all directions over the hemisphere. A dimensionless quantity would therefore only be appropriate if all components of dL_r originating from dE_i were integrated before taking the ratio of dL_r to dE_i. This, however, contradicts the bidirectional concept of the BRDF.

2) Bidirectional Reflectance Factor (BRF): The BRF, also referred to as R, is the radiance dL_r reflected from a surface in a specific direction divided by the radiance dL_{ref} reflected from a lossless, Lambertian reference–reflectance panel measured under identical illumination geometry. The term bidirectional implies that directional measurements should be

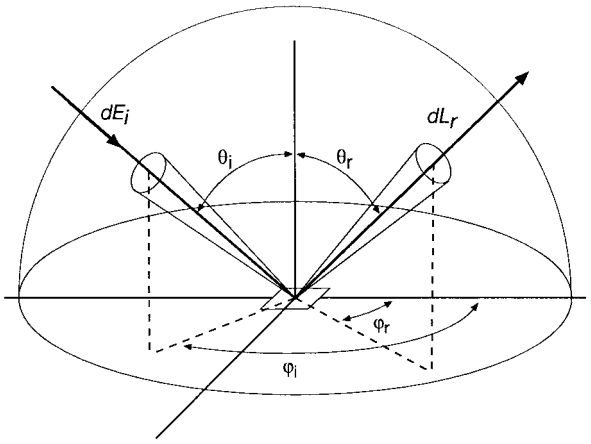

Fig. 7. Concept and parameters of the BRDF.

taken in infinitesimally small solid angles and that illumination from a single direction would be required. Therefore, reflectance factors that are measured are sometimes referred to as biconical reflectance factors. Since the field-of-view of the GER-3700 is sufficiently small and field measurements are taken under clear sky conditions with predominantly direct radiation, the measured values closely approximate BRF's [20]. The deviation of the spectralon reference–reflectance panel from ideal Lambertian reflectance characteristics is corrected with a panel calibration coefficient R_{ref} determined with the GER-3700 radiometer in the laboratory [21]

$$R(\theta_i, \varphi_i; \theta_r, \varphi_r; \lambda) = \frac{dL_r(\theta_i, \varphi_i; \theta_r, \varphi_r; \lambda)}{dL_{ref}(\theta_i, \varphi_i; \theta_r, \varphi_r; \lambda)} R_{ref}(\theta_i, \varphi_i; \theta_r, \varphi_r; \lambda). \quad (2)$$

Unlike BRDF, BRF's are dimensionless. Assuming isotropic irradiance and constant BRDF within designated solid angles, BRDF (f_r) and BRF (R) are interrelated

$$f_r(\theta_i, \varphi_i; \theta_r, \varphi_r; \lambda) = \frac{R(\theta_i, \varphi_i; \theta_r, \varphi_r; \lambda)}{\pi}. \quad (3)$$

Both BRF and BRDF expose values between zero and infinity. Values larger than one for BRF and over $1/\pi$ for BRDF are obtained in peak reflectance directions, such as the hot spot, where the reflected flux from a target surface is higher than the flux from a Lambertian reflector.

3) Anisotropy Factor and Index: Anisotropy factor (ANIF) and anisotropy index (ANIX) are used in this study to analyze the spectral variability in BRDF data. Anisotropy factors (ANIF) allow separation of spectral BRDF effects from the spectral signature of a target. They are calculated by normalizing reflectance data R to nadir reflectance R_0

$$\text{ANIF}(\theta_i, \varphi_i; \theta_r, \varphi_r; \lambda) = \frac{R(\theta_i, \varphi_i; \theta_r, \varphi_r; \lambda)}{R_0(\theta_i, \varphi_i; \lambda)}. \quad (4)$$

The ANIX is an overall estimate for reflectance anisotropy and useful for comparing spectral BRDF effects of different surfaces. It is the ratio of the maximum ($R_{\max}$) and minimum ($R_{\min}$) BRF measured over a target surface in a spectral band

$$\text{ANIX}(\lambda; \theta_i) = \frac{R_{\max}(\lambda)}{R_{\min}(\lambda)}. \quad (5)$$

$R_{\min}$ and $R_{\max}$ are usually located in the solar principal plane. For vegetated surfaces, $R_{\max}$ is associated with the hot spot, whereas $R_{\min}$ is normally close to nadir in the forward scattering direction.

4) Hemispherical Reflectance: Hemispherical reflectance ρ is the ratio of total hemispherical reflected (Φ_r) and incident (Φ_i) radiant flux

$$\rho = \frac{\Phi_r}{\Phi_i}. \quad (6)$$

ρ is sometimes referred to as spectral albedo and derived by integration of the BRF's R over the hemisphere

$$\rho(\theta_i, \varphi_i; \lambda) = \frac{1}{\pi} \int_{\varphi_r=0}^{\varphi_r=2\pi} \int_{\theta_r=0}^{\theta_r=\pi/2} R(\theta_i, \varphi_i; \theta_r, \varphi; \lambda) \cdot \cos(\theta_r) \cdot \sin(\theta_r)\, d\theta_r\, d\varphi_r. \quad (7)$$

B. Measurement Technique and Considerations

1) Measurement Scheme: By default, increments of 15 and 30° are set in the zenith and azimuth directions, respectively. From -75 to $+75$° view zenith angle, 11 target measurements are taken in each of the six azimuth directions from 0 to 150°. Thus, to cover the hemisphere, 66 measurements of the target surface are needed. A measurement series usually starts in the solar principal plane where bidirectional reflectance effects are most pronounced. The alignment of the zenith arc with the sun is accomplished using the engraved azimuth angle scale that is oriented to the geographical north by a compass and verified with the cast shadow of the zenith arc. Subsequently, the zenith arc is rotated by 30° to acquire data in the consecutive azimuth profiles. Each azimuth plane requires about 3 min, resulting in a total data acquisition time of approximately 18 min. In the middle of each azimuth profile, a Spectralon reference–reflectance panel is measured from nadir position to determine irradiance conditions. A support allows precise alignment of the panel with the goniometer's azimuth plane and ensures vertical measurement position (Fig. 3, foreground). The Spectralon panel is corrected for the non-Lambertian and nonideal reflectance characteristics [21]. In addition, a Reagan sunphotometer is usually applied to monitor irradiance conditions and determine the percentage of diffuse irradiance.

2) Considerations of Field-of-View and Irradiance Conditions: The BRDF concept assumes monodirectional viewing and illumination conditions (compare Section III-A). In actual field campaigns, however, the radiometer's field-of-view and the sun's irradiance are not delimited in a single direction. With FIGOS, a directional field-of-view is approximated by choosing a small sensor field-of-view of 3°. Constant and direct illumination can be assumed for short measurement periods and clear sky conditions with low aerosol concentration and lack of clouds. Changes of atmospheric conditions and in the sun's position during data acquisition are largely compensated by frequent reference–reflectance measurements. Since the bulk of diffuse irradiance under clear sky conditions

is circumsolar [22] and thus close to the direction of the direct illumination beam, the influence on BRDF measurements is reasonably small. A sensitivity analysis under controlled laboratory conditions has shown that for FIGOS an optimal compromise between a short measurement time and a high BRDF sampling rate is achieved through the chosen data acquisition scheme described above [21].

3) Sample Size, Heterogeneity, and Representation: Due to the rather small radiometer's field-of-view, the sampling areas of FIGOS are small, particularly, in nadir direction (Fig. 5). In order to obtain representative measurement samples, targets are restricted to relatively small-scale and smooth surfaces, such as dense and homogeneous vegetation canopies, man-made surfaces, and soils. Advantages of small sampling sizes, on the other hand, include better control over environmental conditions and the ability for controlled case studies with distinct sample surfaces. Use of FIGOS to collect BRDF data on small scales still can complete the groundwork required for remote sensing of larger areas since the relation of a grass lawn structure to the FIGOS sampling size for example is analog to observing a forested area with a remote-sensing device of 250-m pixel size.

C. Data Processing and Analysis

The chronologically numbered field measurements are first transferred to a file system that handles different angular sampling resolutions, measurement starting points, and sensor moving directions as well as gaps in the data series. The data are then transformed from a binary into a standard ASCII format. Imported into IDL [23], quality tests for sensor drop outs, sensor noise, and consistency of nadir measurements are performed, followed by the derivation of reflectance values. In order to reduce the impacts of atmospheric and sun position changes, reflectances are determined individually for the six azimuth profiles using the corresponding spectralon reference–reflectance measurements. The non-Lambertian reflectance characteristics of the panel are taken into account according to (2) (Section III-A.). BRDF data, anisotropy factor, and anisotropy index, as well as hemispherical reflectance values are derived based on (3)–(5) and (7). Interpolation techniques as applied in the hot spot direction and for view zenith angles over 75° are described in Sandmeier *et al.* [21], together with plotting algorithms and coordinate systems used.

IV. Field Experiment

A. Experiment Setup

A moderately moist, dense, and uniform soccer grass lawn located at Cham/Zug in Central Switzerland (47°11′36″ N / 8°27′17″ E, 431 m asl) was measured June 14, 1996, between 9:13 and 9:33 UT under clear sky conditions (Fig. 3). During the measurement series, the sun zenith angle began at 35.9° and ended at 33°. The target area was almost completely flat with a tilt angle less than 1°. The predominant species was perennial ryegrass (*Lolium perenne*), with an average canopy height between 3 and 3.5 cm. Measurements and processing steps were completed as described in Section III-B. The sunphotometer was not available for this particular day. Local meteorological stations reported a meteorological visibility range of about 30 km, which corresponds to an aerosol optical thickness of 0.20 at 550 nm and a percentage diffuse irradiance of 19% at 550 nm [24]. The six reflectance–reference measurements taken periodically during data acquisition showed a relative root mean square error (rmse) of 2.1% at 550-nm wavelength after correcting the impact of sun zenith angle changes based on the cosine law. Thus, fairly stable atmospheric conditions can be assumed for the measurement time frame. The GER-3700 experienced sensor dropouts in a few bands and noise problems in wavelength bands below 500 nm, around 1050 nm, and particularly above 1850 nm. Major outliers are excluded from analysis and shown as gaps in the figures. Due to the technical configuration of FIGOS, measurements close to the hot spot are affected by sensor shadow. Thus, the hot spot area is interpolated using a spherical Delaunay triangulation technique described in Sandmeier *et al.* [21]. In line graphs showing the principal plane, only values at +30° view zenith angle are affected.

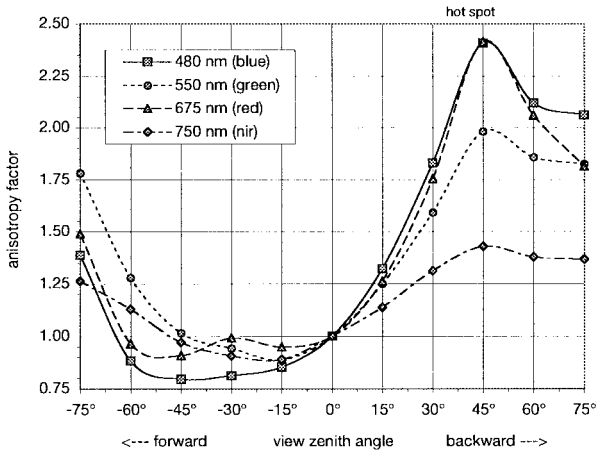

Fig. 8. Anisotropy factors of grass versus view zenith angle in the solar principal plane for four spectral bands. Sun zenith angle is 35°. Values for 30° view zenith angle are interpolated due to the sensor shadow.

B. Results and Discussion

The nadir-normalized[1] BRDF data (i.e., ANIF data) of perennial ryegrass showed a strong spectral variability (Figs. 8–12). In the visible blue and red chlorophyll absorption bands, BRDF effects were pronounced, whereas in the visible green and particularly in the low absorbing near-infrared range, relatively low BRDF effects were observed. This finding is analogous to the results of a laboratory campaign conducted at the European Goniometric Facility (EGO) of the Joint Research Center (JRC) in Ispra, Italy [25]. The spectral dependence of BRDF effects is caused by the relationship between canopy optical properties and multiple scattering effects. In the high absorbing (i.e., low reflecting) wavelength ranges, multiple scattering effects are reduced due to the relatively low amount of radiation in the

[1] We could also choose hemispherical reflectance [Fig. 10(a) and (b)] for normalizing the reflectance data without producing major changes in the results presented.

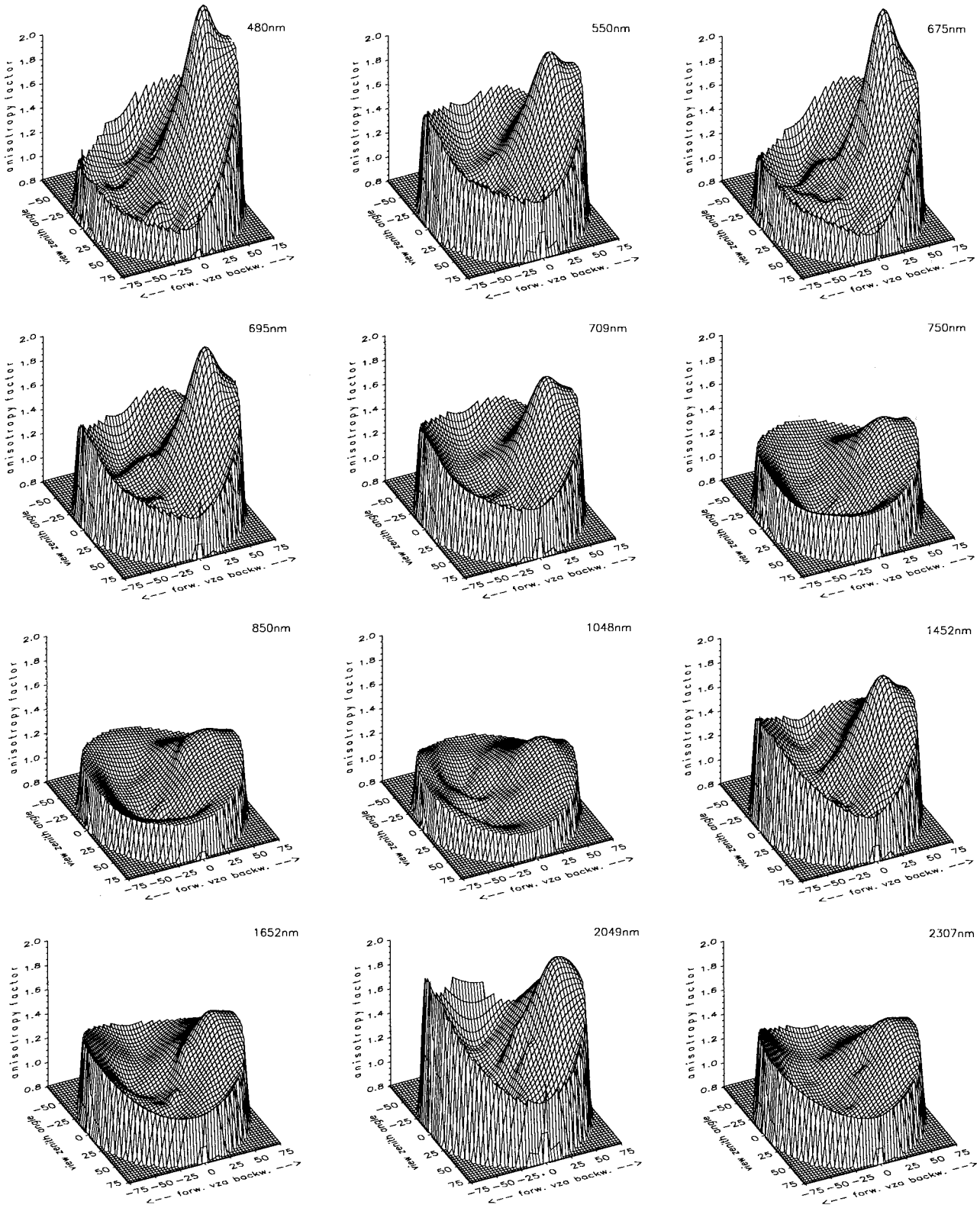

Fig. 9. Anisotropy factors (i.e., nadir-normalized BRDF data) of a grass lawn for 12 representative spectral bands acquired with FIGOS under a sun zenith angle of 35°.

vegetation canopy. Thus, the contrast between shadowed and illuminated canopy components, and subsequently, the BRDF effects are enhanced. In the visible green and, particularly, in the near-infrared range, multiple scattering effects are strong and diminish the contrast in the canopy. As a consequence, BRDF effects are rather small in the low-absorbing (i.e., high-reflecting) wavelength ranges.

Figs. 8–12 illustrate the spectral variability of BRDF effects in ryegrass through five different perspectives. In Fig. 8, anisotropy factors are depicted in the solar principal plane

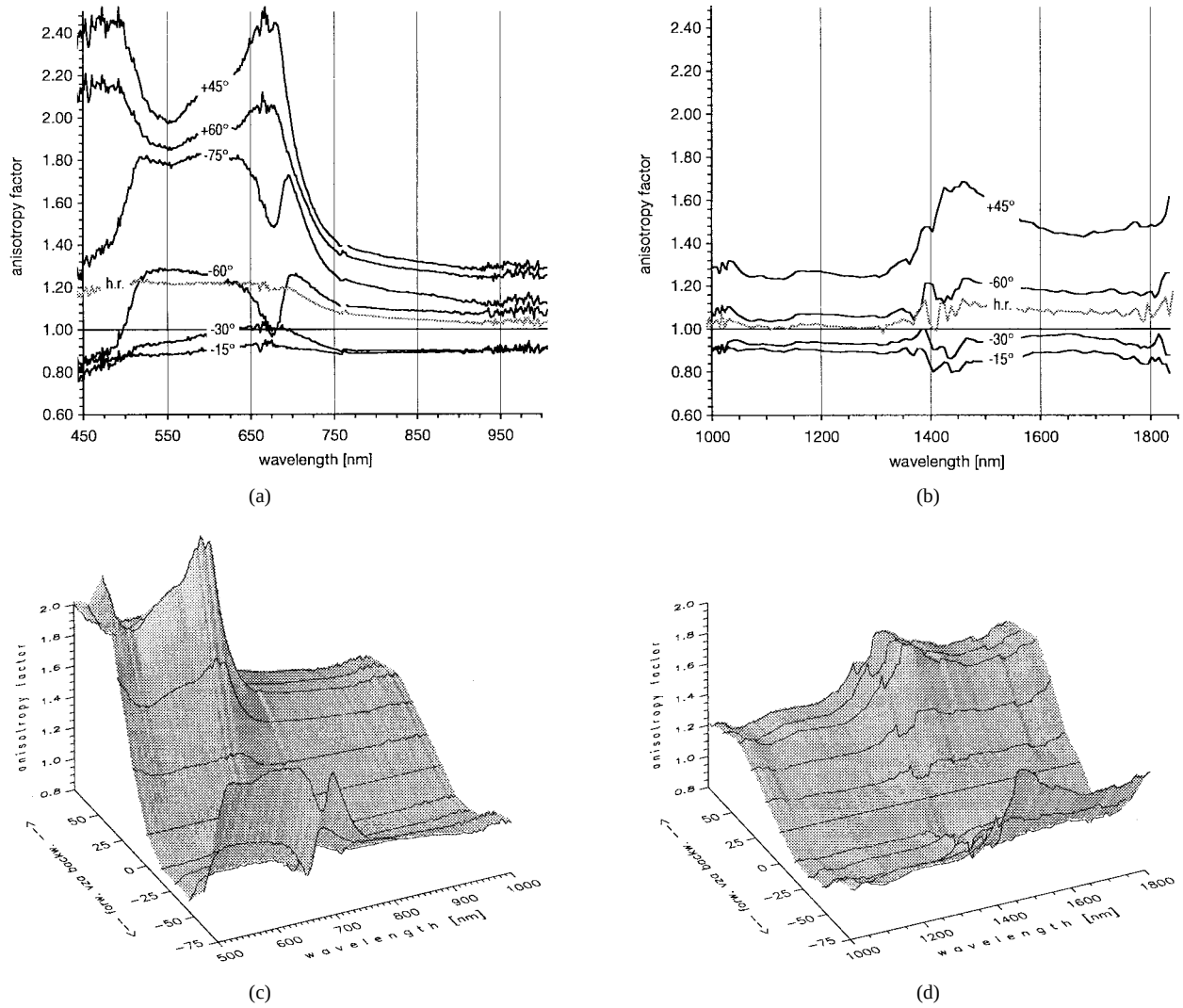

Fig. 10. Anisotropy factors of grass for various view zenith angles in the solar principal plane for two spectral ranges (a), (b) acquired under 35° solar zenith angle. Corresponding 3-D plots are depicted in (c) and (d). Due to the relatively high amount of noise in measurements above 1000 nm, data in (b) and (d) are smoothed with a mean filter function. Values at $+30^{\circ}$ view zenith angle are interpolated since the measurements at this particular position are affected by sensor shadow. Hemispheric reflectance is identified with h.r.

for four wavelength bands representing the colors red, blue, and green and the near-infrared range. Typical for vegetated surfaces, all four bands expose bowl shape, hot spot, and forward scattering components, but the extent of the BRDF features varies significantly among the four wavelengths. In the forward scattering direction, for example, the blue band exhibits much lower anisotropy factors than the green and red bands due to transmittance effects. As a consequence, the color of grass and other vegetated surfaces often show a touch of yellow in the forward scattering direction [26, Fig. 1]. In the hot spot direction, the green reflectance is decreased relative to the reflectance of red and blue wavelengths. Thus, the hot spot appears white rather than green.

The spectral variability of BRDF effects in perennial ryegrass is summarized in Fig. 9 for 12 wavelength bands between 480 and 2307 nm. The first three wavelengths 480, 550, and 675 nm show extremes of the continuously changing BRDF shapes, and the wavelength bands between 675 and 1048 nm illustrate the transition of the BRDF from the high-absorbing visible red to the high-reflecting near-infrared part. Throughout the near-infrared range, the high amount of multiple scattering limits BRDF effects. There are, however, exceptions, such as the 1452- and 2049-nm bands, where lower reflectances cause rather strong BRDF effects due to a decrease in multiple scattering [refer to nadir reflectance signature in Fig. 11(a)]. The hot spot that is interpolated from adjacent measurements [21] emerges particularly in the high-absorbing wavelength ranges, such as the blue and red, but is less pronounced in the highly reflective near-infrared bands. All 12 wavelength bands show a fairly symmetrical bowl shape due to the gap and backshadow effects [5], [25]. The bowl shape is particularly well developed in the near-infrared since the large amount of multiple scattering reduces hot spot and forward scattering components but augments reflectance at high view zenith angles. Forward scattering is still evident in the near infrared when low reflectance values lead to a decrease of multiple scattering effects, such as in the 1452- and 2049-nm bands. In contrast to the visible range, where forward scattering is mostly due to specular reflectance, in the near-infrared, the forward scattering component is caused

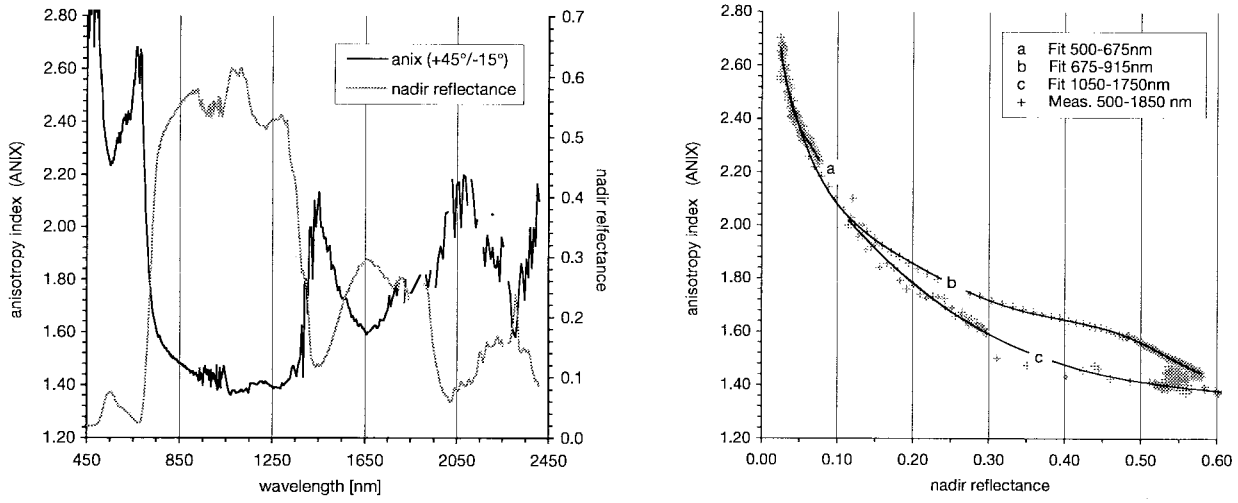

Fig. 11. ANIX versus (a) wavelength and (b) nadir reflectance. ANIX data are the ratio between reflectances at $+45$ and $-15°$ view zenith angles in the solar principal plane in our case. Gaps in the measurement series in (a) are due to sensor drop outs. The polynomial functions used in (b) are of third (500–675 and 1050–1750 nm) and sixth degree (675–915) and expose R2 values of 0.95, 0.99, and 1.00, respectively. Two wavelength ranges, 915–1050 and 1750–1850 nm, are excluded from the polynomial fits to reduce the impact of outliers.

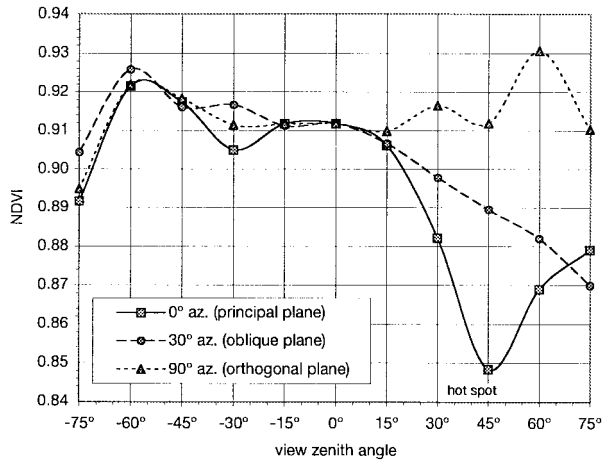

Fig. 12. NDVI for various view zenith angles in three different azimuth planes.

by strong transmittance effects. A further discussion of the spectral dependence of the bowl shape, hot spot, and forward scattering components is given in Meister *et al.* [27].

Continuity in BRDF changes over the spectral range is demonstrated for principal plane data in Fig. 10. Fig. 10(a) and (b) provide a more quantitative analysis, while Fig. 10(c) and (d) emphasize the persistence of the BRDF effect over the various view zenith angles. Fig. 11 confirms that most of the spectral variations of the BRDF are related to surface reflectance, which dominates multiple scattering in a vegetation canopy. The fact that the ANIF data for different wavelength ranges do not overlay in Fig. 11(b) is believed to be caused by leaf transmittance effects that are not always linearly correlated with canopy reflectance properties and therefore contribute an additional component to the multiple scattering effect [25].

The spectral variability of BRDF effects also has a major impact on normalized difference vegetation index (NDVI) products since they are derived from two wavelengths with completely different BRDF characteristics (Fig. 12) [28]. The red band exposes very high BRDF dynamics, whereas in the near-infrared, BRDF effects are rather small (Fig. 9). The highest impact is evident in the hot spot area where a 7% decrease of NDVI from nadir NDVI results from BRDF effects in our case (Fig. 12). For higher source zenith angles even larger deviations are expected since the BRDF effect is more pronounced under high solar zenith angles [5].

V. Conclusions

A unique field goniometer system, FIGOS, has been developed for the acquisition of hyperspectral BRDF data of small-scale surfaces under natural illumination conditions. FIGOS is a transportable instrument that collects hemispherical BRDF data sets in approximately 18 min with a positioning accuracy of $\pm 0.2°$ in zenith and azimuth directions. Field campaign data taken from perennial ryegrass at 35° solar zenith angle revealed a strong spectral variability of BRDF effects. The ratio between the maximum and minimum reflectance measurements over the hemisphere, defined as ANIX in this study, varied between 1.4 and 2.8 for the 450–2450-nm wavelength range (excluding outliers). In agreement with laboratory results [25], most of the spectral variations in the BRDF of perennial ryegrass are related to the target surface reflectance that controls a large amount of multiple scattering, and, as a consequence, affects the contrast between shadowed and sunlit canopy components. Wavelength ranges with high reflectance showed strong multiple scattering effects and diminished the BRDF effect. Ranges with low surface reflectance, however, exhibited low multiple scattering and pronounced BRDF effects. Consequently, NDVI products are biased by spectral BRDF effects.

Since multiple scattering effects are ultimately related to canopy structure, hyperspectral BRDF data have a potential for derivation of canopy architecture parameters, such as the leaf angle index (LAI) and the leaf area distribution (LAD)

from remote-sensing data [26]. Integration of the spectral variability of BRDF effects into remote-sensing applications, however, still requires further ground work and modeling efforts to improve our understanding of the physics behind BRDF effects.

ACKNOWLEDGMENT

The FIGOS goniometer development would not have been possible without the know-how and dedication of its constructor W. Sandmeier and the generous technical and financial support of Fa. Lehner & Co. AG, Gränichen, Switzerland. The Laboratory of the Physics Department at the University of Zürich, Switzerland, contributed additional technical support.

REFERENCES

[1] B. Hosgood, S. Sandmeier, J. Piironen, G. Andreoli, and C. Koechler, "Goniometers," *Encyclopedia of Electrical and Electronics Engineering.* New York: Wiley, in press.
[2] F. E. Nicodemus, J. C. Richmond, J. J. Hsia, I. W. Ginsberg, and T. Limperis, "Geometrical considerations and nomenclature for reflectance," *Nat. Bur. Standards Mono.*, vol. 160, no. 52, Oct. 1977.
[3] K. L. Coulson, G. M. Bouricius, and E. L. Gray, "Optical reflection properties of natural surfaces," *J. Geophys. Res.*, vol. 70, no. 18, pp. 4601–4611, 1965.
[4] H. T. Breece and R. A. Holmes, "Bidirectional scattering characteristics of healthy green soybean and corn leaves *in vivo*," *Appl. Opt.*, vol. 10, no. 1, pp. 119–127, 1971.
[5] D. S. Kimes, "Dynamics of directional reflectance factor distributions for vegetation canopies," *Appl. Opt.*, vol. 22, no. 9, pp. 1364–1372, 1983.
[6] D. W. Deering and P. Leone, "A sphere-scanning radiometer for rapid directional measurements of sky and ground radiance," *Remote Sens. Environ.*, vol. 19, pp. 1–24, 1986.
[7] R. D. Jackson, P. M. Teillet, P. N. Slater, G. Fedosejevs, M. F. Jasinski, J. K. Aase, and M. S. Moran, "Bidirectional measurements of surface reflectance for view angle corrections of oblique imagery," *Remote Sens. Environ.*, vol. 32, pp. 189–202, 1990.
[8] E. A. Walter-Shea, C. J. Hays, M. A. Mesarch, and R. D. Jackson, "An improved goniometer system for calibrating field reference-reflectance panels," *Remote Sens. Environ.*, vol. 43, pp. 131–138, 1993.
[9] J. L. Privette, D. W. Deering, and D. E. Wickland, "Report on the workshop on multiangular remote sensing for environmental applications," NASA Tech. Memo., vol. 113202, no. 50, Oct. 1997.
[10] C. J. Readings and M. L. Reynolds, "Reports for assessment, the nine candidate Earth Explorer missions," Eur. Space Agency, vol. SP-1196, no. 2, 1996.
[11] T. Cooley, G. Seigel, I. Thorson, J. Olson, and M. Stoyanof, "Warfighter-1: An air force partnership with industry to advance space imaging spectroscopy," in *Proc. 35th Space Congr.*, II C-S, Cocoa Beach, FL, 1998.
[12] A. Ginati, C. Tobehn, A. Blasberger, J. Topaz, and A. Karnieli, "DAVID—A multi spectral high resolution small satellite," in *Proc. 11th AIAA/USU Conf. Small Satellites*, Utah State Univ., Logan, SSC97-III-3, 1997.
[13] D. W. Deering, E. M. Middleton, J. R. Irons, B. L. Blad, E. A. Walter-Shea, C. J. Hays, C. Walthall, T. F. Eck, S. P. Ahmad, and B. P. Banerjee, "Prairie grassland bidirectional reflectances measured by different instruments at the FIFE site," *J. Geophys. Res.*, vol. 97, no. D17, pp. 18 887–18 903, 1992.
[14] C. A. Russell, J. R. Irons, and P. W. Dabney, "Bidirectional reflectance of selected BOREAS sites from multiangle airborne data," *J. Geophys. Res.*, vol. 102, no. D24, pp. 29 505–29 516, 1997.
[15] C. A. Russell, C. L. Walthall, J. R. Irons, and E. C. Brown de Colstoun, "Comparison of airborne and surface spectral bidirectional reflectance factors, spectral hemispherical reflectance and spectral vegetation indices," *J. Geophys. Res.*, vol. 100, no. D12, pp. 25 509–25 522, 1997.
[16] K. J. Ranson, J. R. Irons, and D. L. Williams, "Multispectral bidirectional reflectance of northern forest canopies with the advanced solid-state array spectroradiometer (ASAS)," *Remote Sens. Environ.*, vol. 47, pp. 276–289, 1994.
[17] E. M. Middleton, "Quantifying reflectance anisotropy of photosynthetically active radiation in grasslands," *J. Geophys. Res.*, vol. 97, no. D17, pp. 18 935–18 946, 1992.
[18] GER, GER-3700 Spectroradiometer, User's Manual Version 2.0, Geophys. Environ. Res. Corp., Millbrook, NY, 59, 1997.
[19] S. Sandmeier, W. Sandmeier, K. I. Itten, M. E. Schaepman, and T. W. Kellenberger, "Acquisition of bidirectional reflectance data using the Swiss field-goniometer system (FIGOS)," in *Proc. EARSeL Symp.*, Basel, Switzerland, Balkema Publ. NL, 1995, pp. 55–61.
[20] B. F. Robinson and L. L. Biehl, "Calibration procedures for measurement of reflectance factor in remote sensing field research," in *Proc. Soc. Photo-Opt. Instrum. Eng., 23rd Annu. Tech. Symp. Measure. Opt. Radiat., SPIE*, Bellingham, WA, 1979, pp. 16–26.
[21] S. Sandmeier, C. Müller, B. Hosgood, and G. Andreoli, "Sensitivity analysis and quality assessment of laboratory BRDF data," *Remote Sens. Environ.*, vol. 64, no. 2, pp. 176–191, 1998a.
[22] S. Sandmeier and K. I. Itten, "A physically-based model to correct atmospheric and illumination effects in optical satellite data of rugged terrain," *IEEE Trans. Geosci. Remote Sensing*, vol. 35, pp. 708–717, May 1997.
[23] RSI, IDL Version 5.0, Reference and User's Guide, Res. Syst., Inc., Boulder, CO, 1997.
[24] E. F. Vermote, D. Tanré, J. L. Deuzé, M. Herman, and J.-J. Morcrette, "Second simulation of the satellite signal in the solar spectrum, 6S: An overview," *IEEE Trans. Geosci. Remote Sensing*, vol. 35, pp. 675–686, May 1997.
[25] S. Sandmeier, C. Müller, B. Hosgood, and G. Andreoli, "Physical mechanisms in hyperspectral BRDF data of grass and watercress," *Remote Sens. Environ.*, vol. 66, no. 2, pp. 222–233, 1998.
[26] S. Sandmeier, E. M. Middleton, D. W. Deering, and W. Qin, "The potential of hyperspectral BRDF data for grass canopy characterization," *J. Geophys. Res.*, in press.
[27] G. Meister, St. Sandmeier, and W. Ni, "Analyzing hyperspectral BRDF data of a grass lawn and watercress surface using an empirical model," in *Proc. IGARSS'98*, Seattle, WA, pp. 1246–1248.
[28] L. F. Johnson, "Multiple view zenith angle observations of reflectance from ponderosa pine stands," *Int. J. Remote Sensing*, vol. 15, no. 18, pp. 3859–3865, 1994.

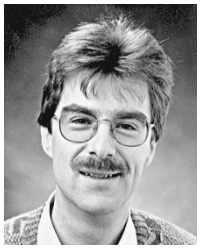

Stefan R. Sandmeier received the M.Sc. and Ph.D. degrees in 1991 and 1995, respectively, both from the University of Zürich, Zürich, Switzerland.

He was a Research Scientist and Project Manager at the Remote Sensing Laboratories, Department of Geography, University of Zürich. Since 1997, he has been a Postdoctoral Fellow at the Biospheric Sciences Branch, NASA/Goddard Space Flight Center, Greenbelt, MD. He investigated the radiometric corrections of topographically induced effects on Landsat TM data in an alpine environment and assessed the improvements in land cover classifications that resulted. He also led in the development and evaluation of the Swiss Field Goniometer System (FIGOS), the acquisition of bidirectional reflectance data using this system, and the performance of sensitivity studies on these bidirectional reflectance data. His current interest includes spectral variability of bidirectional reflectance effects and its application in ecologically relevant studies.

Klaus I. Itten received the M.Sc. and Ph.D. degrees in geography from the University of Zürich, Zürich, Switzerland, in 1969 and 1973, respectively.

He was with NASA/Goddard Space Flight Center, Greenbelt, MD, in 1974 as a Research Fellow of the European Space Agency. In 1982, he was an Assistant Professor and has acted since 1988 as a Full Professor in geography and since 1998 as a Director of the Department of Geography at the University of Zürich-Irchel, where he is also heading the Remote Sensing Applications Division of the Remote Sensing Laboratories. His research and teaching interests include remote sensing and image processing for natural resources inventorying and monitoring.

Dr. Itten is past President of the Swiss Remote Sensing Commission, a member of the Swiss Commission on Space Research, a member of the Federal Commission of Space Affairs, and acts as the Swiss Delegate to the ESA Data User Programme Advisory Committee (DUP).